



LABORATORY OF FLUID MECHANICS AND TURBOMACHINERY
DEPARTMENT OF MECHANICAL ENGINEERING
UNIVERSITY OF THESSALY, GREECE

**NUMERICAL STUDY OF THE INTERACTION BETWEEN AN
ENCAPSULATED MICROBUBBLE AND A RIGID WALL IN A
VISCIOUS FLOW**

Vlachomitrou Maria & Pelekasis Nikos



European Union
European Social Fund



MINISTRY OF EDUCATION & RELIGIOUS AFFAIRS
MANAGING AUTHORITY

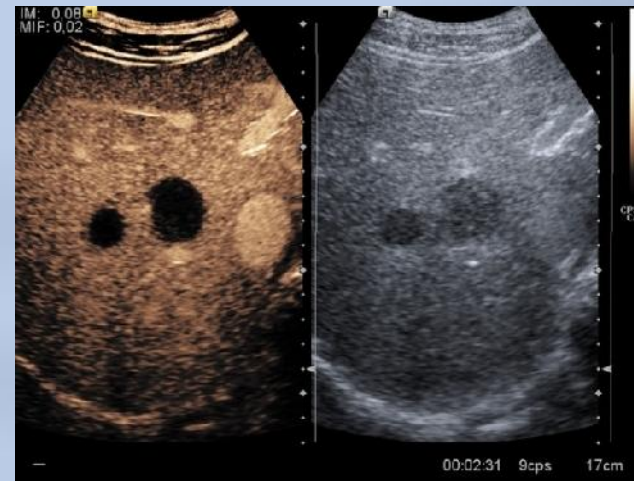
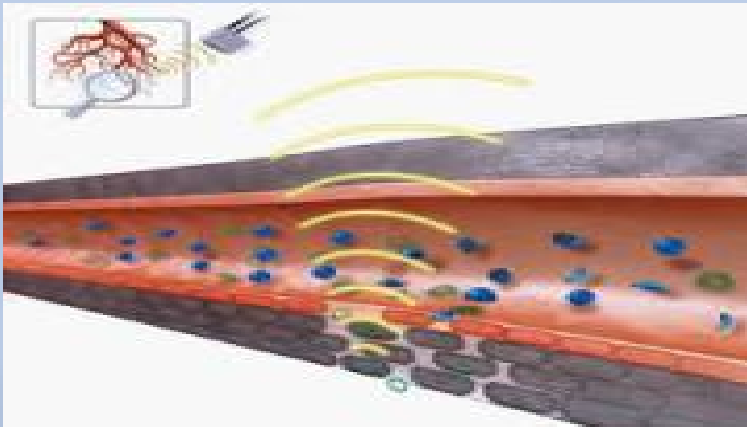
Co-financed by Greece and the European Union



APPLICATIONS

Contrast agents have a wide range of technological applications:

- Targeted drug delivery - encapsulated microbubbles that carry drugs are attached to the affected site and then ruptured by using an appropriate acoustic disturbance (*Ferrera et al., 2007*)
- Medical imaging of vital organs – gas-filled microbubbles are used which are able to enhance the ultrasound backscatter and produce high quality images (*Kaufmann et al., 2007*)

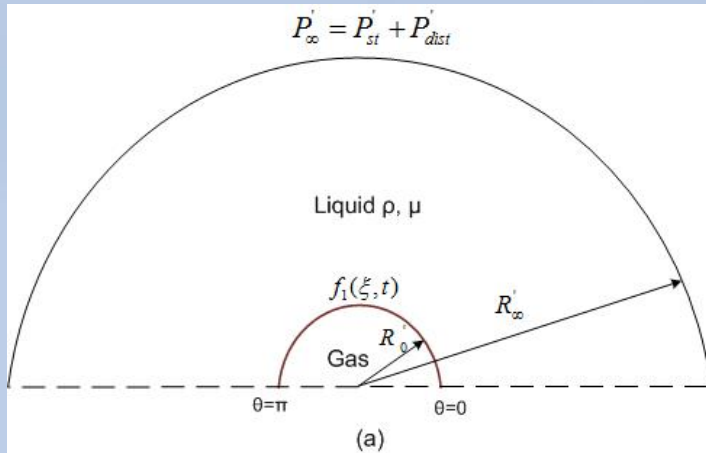


OBJECTIVES

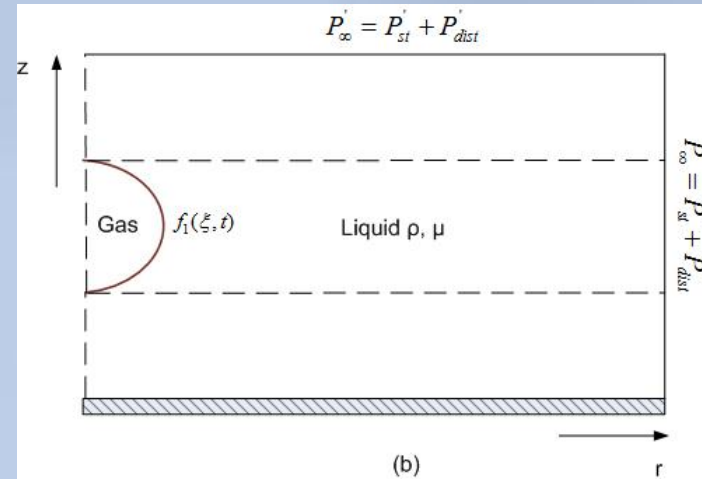
- **Study the response of encapsulated microbubbles to step change and acoustic disturbances when the viscous forces of the surrounding liquid are accounted for.**
- **Determine the effect that the rigid wall has on the behavior of contrast agents.**
- **Define the mechanism that leads to contrast agent collapse – explore the possibility of jet formation**
- **Develop the appropriate numerical methodology for simulating the problem under investigation.**

PROBLEM FORMULATION

Bubble in an unbounded flow



Bubble – wall interaction



Characteristic scales

Length: R_0' , Time: $1/\check{S}_f'$, Velocity: $\check{S}_f' R_0'$, Pressure: $\dots \check{S}_f'^2 R_0'^2$

Continuity equation:

$$\bar{\nabla} \cdot \bar{u} = 0, \quad \text{where } \bar{u} = (u_r, u_\theta, 0) \quad \text{or} \quad \bar{u} = (u_r, u_z, 0)$$

Navier Stokes equation:

$$\frac{\partial \bar{u}}{\partial t} + (\bar{u} \cdot \bar{\nabla}) \bar{u} = -\bar{\nabla} p + \frac{1}{\text{Re}} \bar{\nabla} \cdot \bar{\tau} \quad \text{where } \text{Re} = \frac{\dots \check{S}_f' R_0'^2}{\dots}$$

Kinematic condition:

$$\bar{u} = \frac{D \bar{r}_s}{Dt}$$

Force balance equation:

$$\left(-\frac{PI}{\text{Re}} + \frac{1}{\text{Re}} \underline{\underline{\dagger}} \right) \cdot \bar{n} + P_G \cdot \bar{n} = \frac{(\bar{\nabla}_s \cdot \bar{n}) \bar{n}}{We} + \Delta F = \frac{2k_m}{We} \bar{n} - \bar{\nabla}_s \cdot \underline{\underline{\dagger}}_{el} = -\bar{\nabla}_s \cdot \left(\underline{\underline{\dagger}}_{el} + \frac{1}{We} \underline{\underline{I}} \right)$$

where $We = \dots \check{S}_f^2 R_0^3 / \dagger$

\bar{n} : the normal unit vector pointing inward the liquid fluid

P_G : the gas pressure

$\bar{\nabla}_s, k_m$: the surface gradient and mean curvature on the bubble interface

$-\bar{\nabla}_s \cdot \underline{\underline{\dagger}}_{el}$: the force due to the viscoelastic properties of the membrane

$$-\bar{\nabla}_s \cdot \underline{\underline{\dagger}}_{el} = \left[k_s \dagger_s + k_w \dagger_w - \frac{1}{r_0} \frac{\partial}{\partial S} (r_0 q) \right] \bar{n} - \left[\frac{\partial \dagger_s}{\partial S} + \frac{1}{r_0} \frac{\partial r_0}{\partial S} (\dagger_s - \dagger_w) + k_s q \right] \bar{e}_s$$

\dagger_s, \dagger_w : the principal tensions

\bar{e}_s : the tangential unit vector

q : the transverse shear tension that is obtained from a torque balance on the shell

$$q = \frac{1}{r_0} \frac{\partial r_0}{\partial S} \left[\frac{\partial}{\partial r_0} (r_0 m_s) - m_w \right] \quad \text{where } m_s, m_w \text{ the principal bending moments}$$

The viscoelastic behavior of the membrane is described by the Mooney-Rivlin constitutive law

Adiabatic change of bubble pressure:

$$P_G(t=0) V_G^x(t=0) = P_G(t) V_G^x(t) \quad \text{where } P_G(t=0) = P_{st} + \frac{2}{We}$$

NUMERICAL METHODOLOGY

- Numerical solution is done with the Finite Element Methodology. A superparametric hybrid scheme is employed that combines lagrangian (biquadratic and bilinear) basis functions for the simulation of velocity and pressure in conjunction with 1D cubic splines for the simulation of the interface .

$$\bullet \iiint B_{l,i} \bar{\nabla} \cdot \bar{u} dV = 0$$

$$\bullet \iiint B_i \frac{\partial \bar{u}}{\partial t} \cdot \bar{e}_k dV + \iiint B_i (\bar{u} \cdot \bar{\nabla}) \bar{u} \cdot \bar{e}_k dV - \iiint p \bar{\nabla} (B_i \bar{e}_k) dV + \frac{1}{\text{Re}} \iiint \bar{\ddagger} : \bar{\nabla} (B_i \bar{e}_k) dV + \int B_i \bar{N} \cdot (p \bar{I} - \frac{1}{\text{Re}} \bar{\ddagger} \cdot \bar{e}_k) dA = 0$$

where $\bar{e}_k = (\bar{e}_r, \bar{e}_\theta)$ or $\bar{e}_k = (\bar{e}_r, \bar{e}_z)$

- The kinematic equation is used as essential boundary condition for the velocity, whereas the force balance equation is used for the calculation of the bubble shape (due to the presence of a 4th order partial derivative in the force balance equation).

$$\bullet \int b_i \left(-p \bar{I} + \frac{1}{\text{Re}} \bar{\ddagger} \right) \cdot \bar{n} \cdot \bar{e}_m ds + \int b_i P_G \cdot \bar{n} \cdot \bar{e}_m ds - \int b_i \frac{2k_m}{\text{We}} \bar{n} \cdot \bar{e}_m ds + \int b_i \bar{\Delta F} \cdot \bar{e}_m ds = 0$$

where $\bar{e}_m = (\bar{n}, \bar{e}_s)$ and b_i the cubic spline basis functions

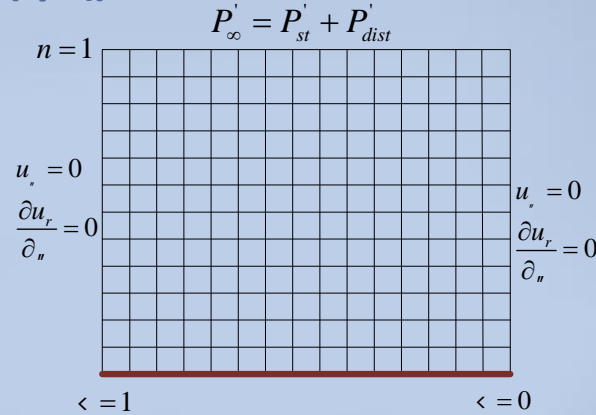
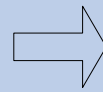
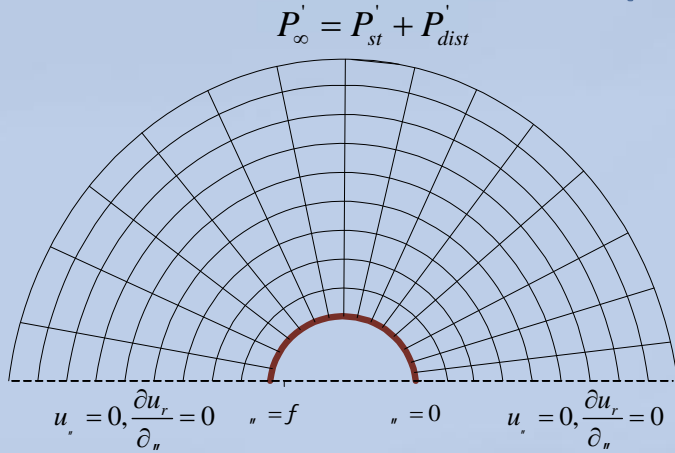
- Time integration is done with a fully implicit Euler scheme.
- The non-linearity of the problem is treated with the Newton-Raphson method.
- The linearised system of equations is solved iteratively with the GMRES method.

GRID CONSTRUCTION

1. SPINE METHOD

The complex physical domain is converted to a simple rectangular computational domain via appropriate variable transformations

Bubble in an unbounded flow $(r, \theta) \longrightarrow (\eta, \xi)$



r-direction:

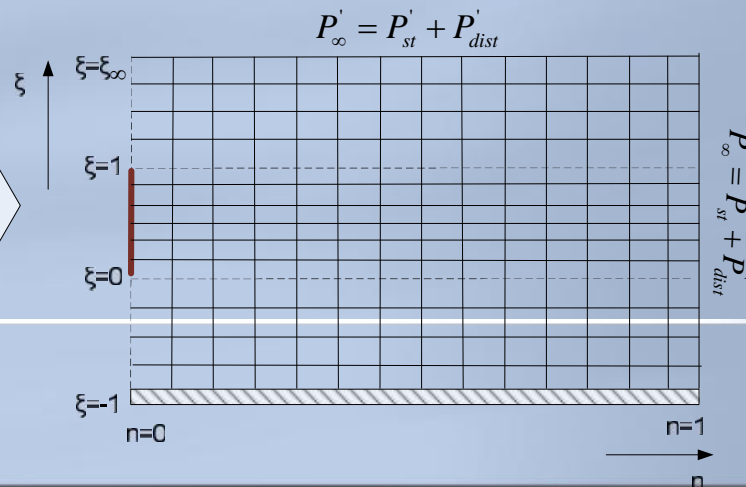
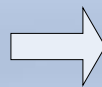
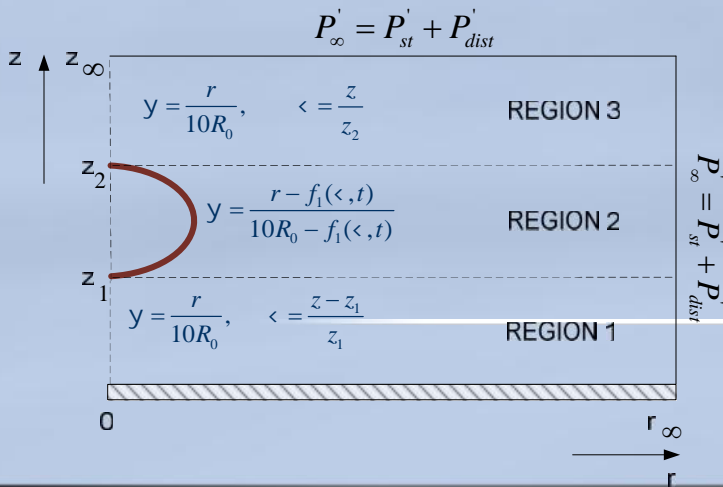
$$y = \frac{r - f_1(\langle, t)}{10R_0 - f_1(\langle, t)}$$

theta-direction:

lagrangian particles

$$\eta = f_2(\langle, t), \quad 0 \leq \langle \leq 1$$

Bubble - wall interaction $(r, z) \longrightarrow (\eta, \xi)$



2. ELLIPTIC MESH GENERATION

(Christodoulou & Scriven, 1992 ; Tsiveriotis & Brown, 1992; Notz & Basaran, 2004)

VARIABLE TRANSFORMATION: (r, z, t) or $(r, \theta, t) \xrightarrow{|J|} (\eta, \xi, t)$

(Dimakopoulos & Tsamopoulos, 2003a)

$$\begin{aligned} \bar{\nabla} \cdot \{ (v_1 S + (1-v_1)) \bar{\nabla} \langle \} &= 0 \quad (\text{n-curves}) \\ \bar{\nabla} \cdot \bar{\nabla} n &= 0 \quad (\xi\text{-curves}) \end{aligned}$$



$$\begin{aligned} \iint (\varepsilon_1 S + (1-\varepsilon_1)) \bar{\nabla} \xi \cdot \bar{\nabla} B_i d\Omega &= 0 \\ \iint \bar{\nabla} n \cdot \bar{\nabla} B_i d\Omega &= 0 \end{aligned}$$

$$S = \sqrt{\frac{r_c^2 + z_c^2}{r_n^2 + z_n^2}} \quad \text{or} \quad S = \sqrt{\frac{r_c^2 + r_{n,c}^2}{r_n^2 + r_{n,n}^2}}$$

- S is introduced in order for the n-curves to be almost perpendicular to the interface.
- ε_1 is an empirical parameter between 0 and 1 that controls the smoothness of the mapping relative to the degree of orthogonality of the mesh lines.
- The penalty method is used wherever we need to control the node distribution

penalty method

$$\iint (v_1 S + (1-v_1)) \bar{\nabla} \langle \cdot \bar{\nabla} B_i d\Omega + L \int \frac{\partial B_i}{\partial \xi} \sqrt{F(\xi)} d\xi = 0$$

where $L \sim O(10^3 - 10^5)$, $w_1 + w_2 = 2$,
 $F(\langle) = w_1 r_c^2 + w_2 r_{n,c}^2$ or $F(\langle) = w_1 r_c^2 + w_2 r_{n,n}^2$

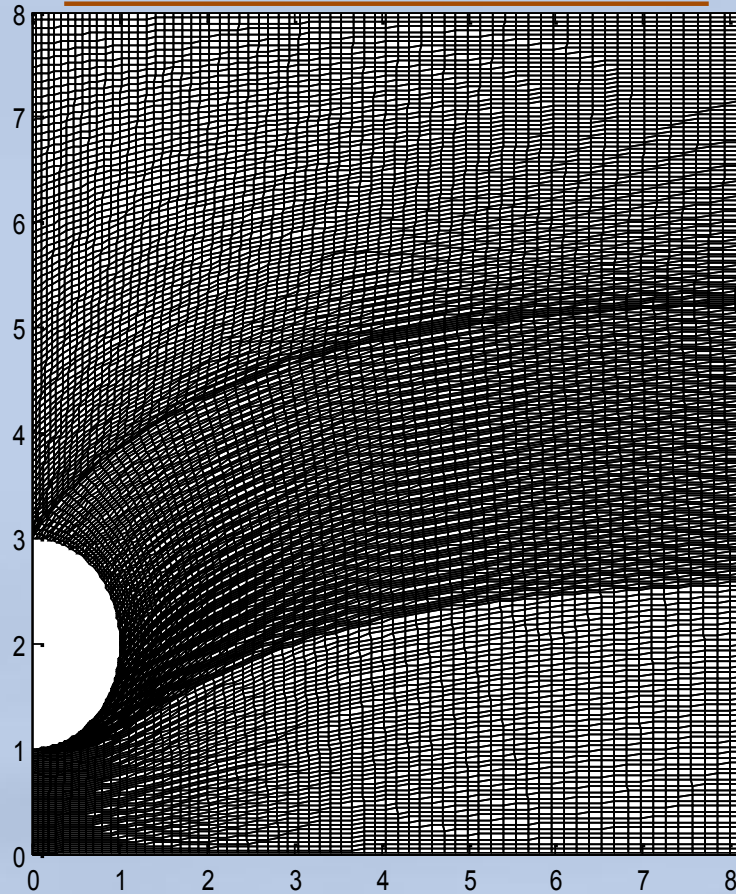
In the presence of a wall the penalty method is applied on the n-curves that starts from the bubble 's poles. (Chatzidai et al., 2009)

Elliptic mesh generation for contrast agents

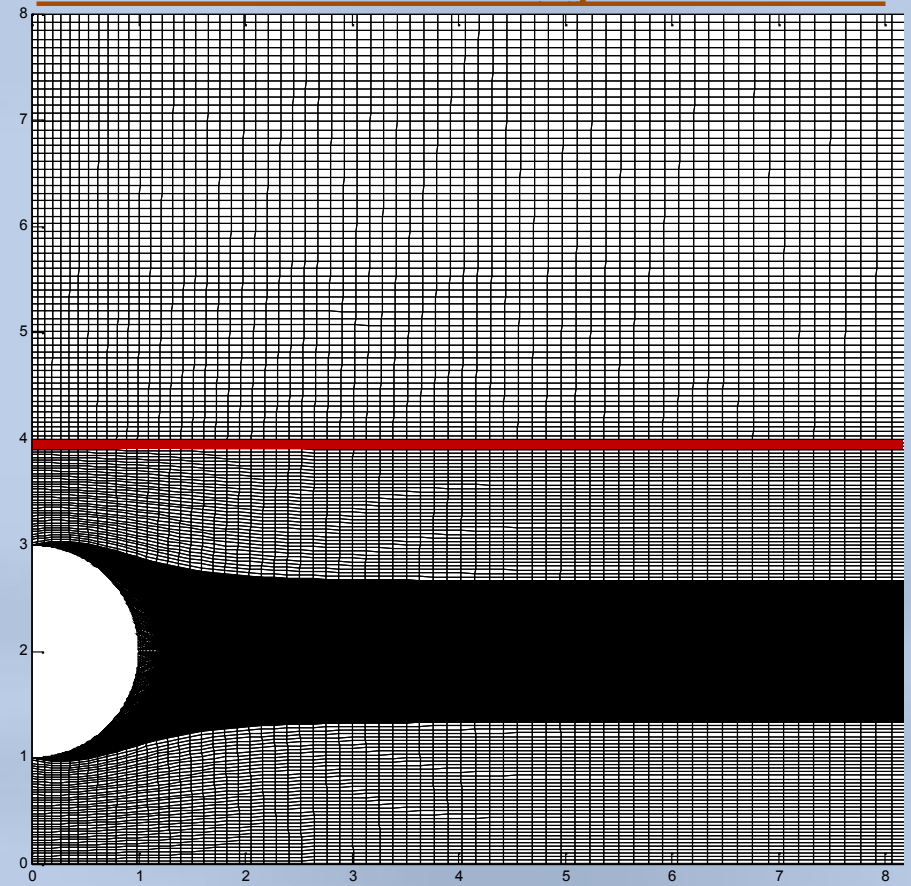
- For the mesh construction we use a hybrid scheme that combines the lagrangian basis functions with the 1D cubic splines. So, the nodes on the interface are described via spline basis functions and all the others nodes with lagrangian functions (*due to the presence of a 4th order partial derivative in the force balance equation*)
- In every time step:
 - a) we solve simultaneously the flow equations and the shape of the interface. This procedure is the same as in the case of the spine method.
 - b) The shape of the interface is used as essential boundary condition to solve the elliptic equations for the grid
- The penalty method is not applied on the interface, but only on the n-curves which start from the bubble poles (in the case of wall presence).
- In all boundaries (except the interface) we impose orthogonality conditions without including the line integrals resulting from the divergence theorem.

- When the bubble gets close to the wall n-grid lines (lines parallel to the wall) tend to pull away from the wall – The grid construction must be done by dividing the area in two separate sub-domains.

Grid construction in one domain

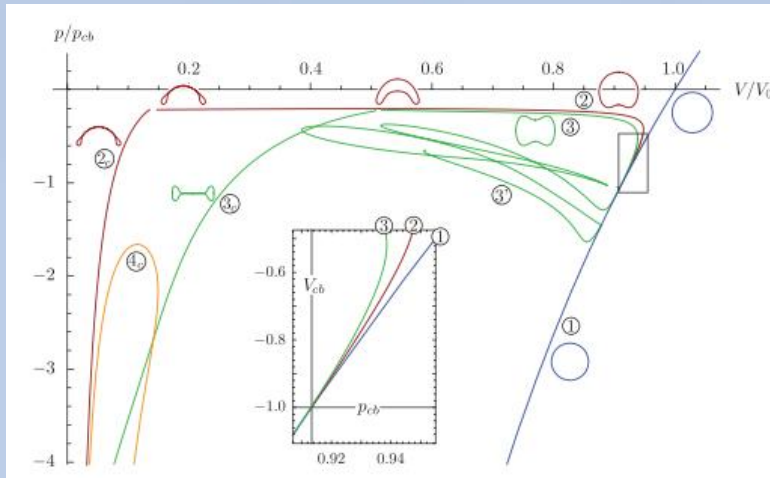


Grid construction in two separate domains

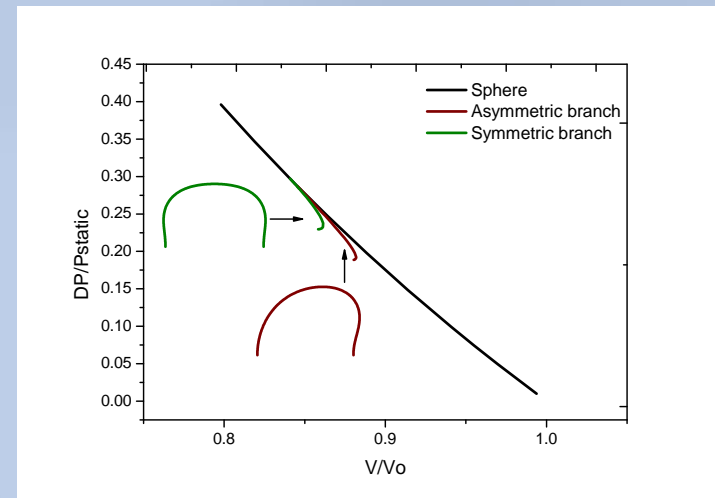


RESULTS FOR STEP CHANGE DISTURBANCES

- For step change disturbances, according to static analysis, contrast agents may reach a static non-spherical state.



(Knoche & Kierfeld, 2011)



(Lytra & Pelekasis, 2014)

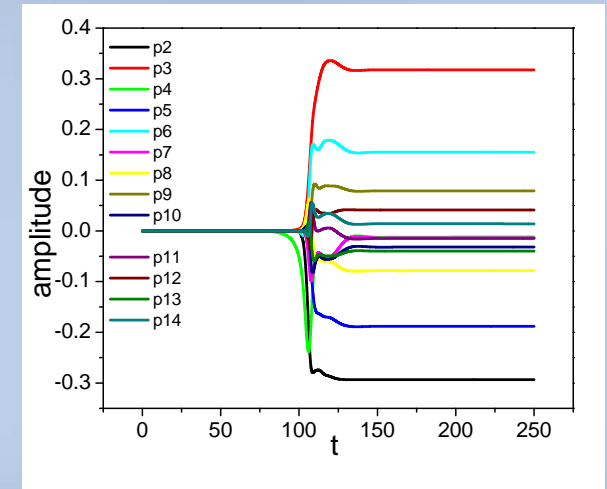
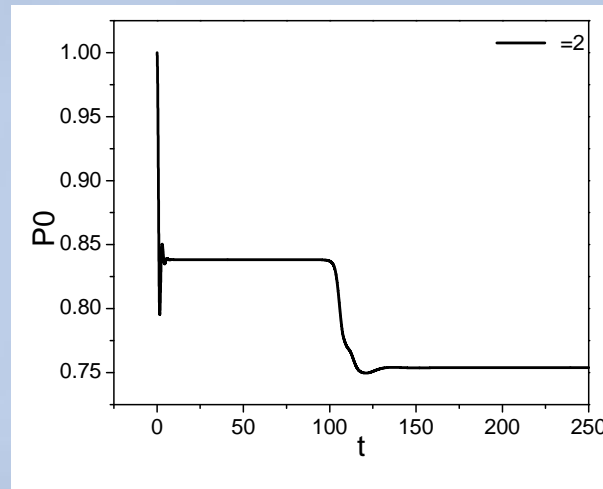
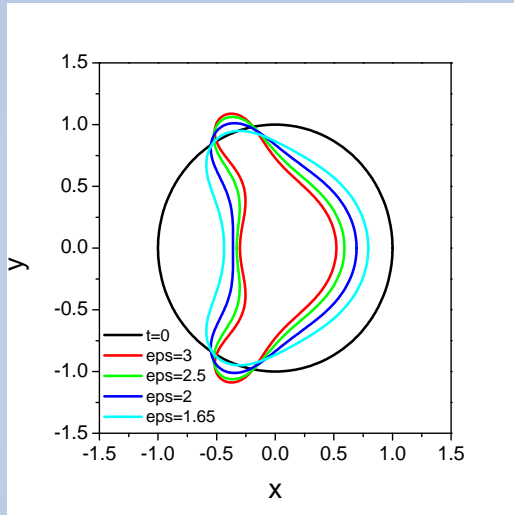
- We are interested in examining the dynamic response of coated microbubbles and investigate the possibility for a static solution to be achieved.
- It is also important to study the response of contrast agents to greater disturbances and determine whether a jet is formed (as it happens in the case of free bubbles).
- It is, also, important to study how the wall presence alters the behavior of contrast agents.

RESULTS FOR STEP CHANGE DISTURBANCES IN AN UNBOUNDED FLOW

$R_0' = 3.6 \mu\text{m}$, $\mu_s = 20 \text{Pa}\cdot\text{s}$, thickness = 1nm , $G_s = 80 \text{MPa}$, $k_b = 3 \cdot 10^{-14} \text{N}\cdot\text{m}$
 $\rho = 998 \text{kg}/\text{m}^3$, $\mu = 10^{-3} \text{Pa}\cdot\text{s}$, $\sigma = 0.051 \text{N}/\text{m}$, $\gamma = 1.07$

Surrounding liquid:
 water ($\mu_l = 10^{-3} \text{Pa}\cdot\text{s}$)

External disturbance: $P_\infty' = P_{st}' [1 + \nu]$, $\nu = 1.65 - 3$



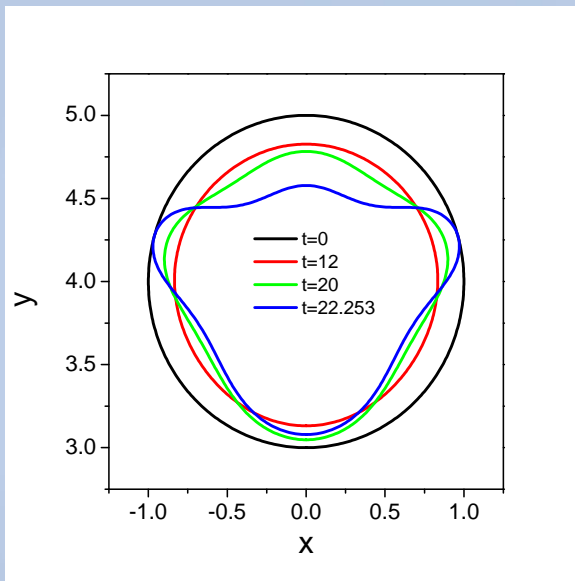
- The bubble performs few volume pulsations and reaches a compressed spherical shape – For amplitudes $\epsilon > 1.65$ static buckling is observed ($\epsilon_{cr} = 1.55$)
- Finally, for $\epsilon = 1.65 - 3$, a new non-spherical static solution is reached that has smaller energy than the intermediate spherical one.
- If the viscosity of the surrounding liquid is reduced the same static solution is obtained.
- If we ignore the viscosity of the liquid or the surface tension or if we don't permit the movement of the bubble, the non-spherical state is not observed. Shape modes grow continuously and the bubble eventually collapses.

RESULTS FOR STEP CHANGE DISTURBANCES FOR THE BUBBLE-WALL INTERACTION

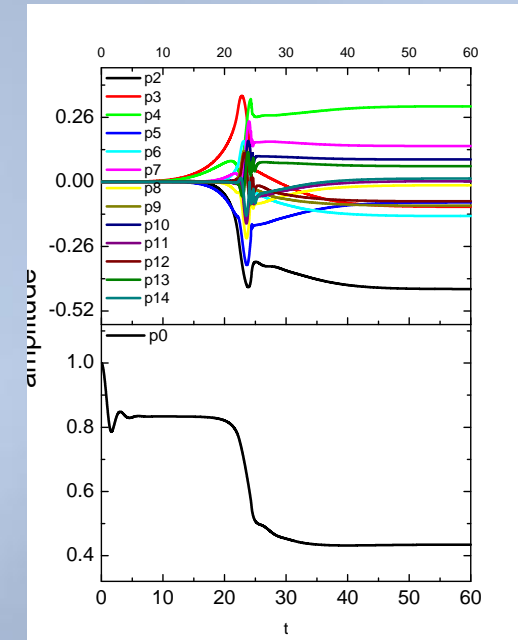
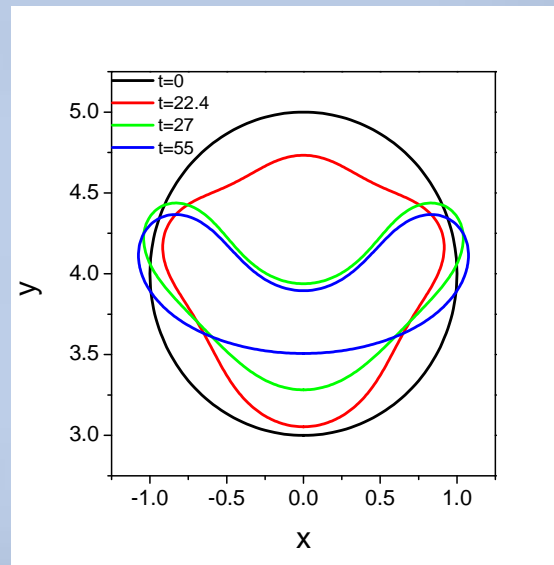
- External disturbance: $P'_\infty = P'_{st} [1 + \nu], \nu = 2$
- Distance between the lower pole and the wall: $z_1 = 3$

Surrounding liquid:
Water ($\mu_l = 10^{-3} Pa \cdot s$)

Spine method



Elliptic method



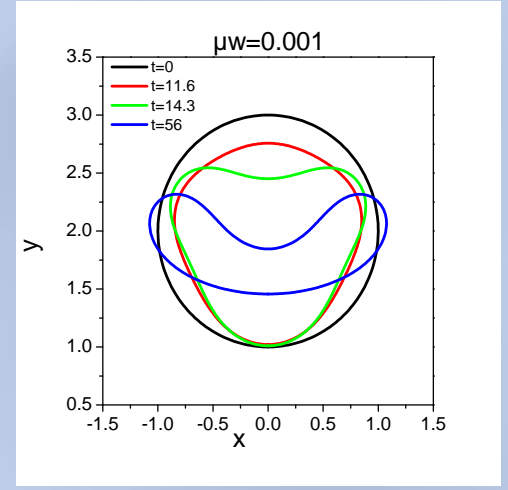
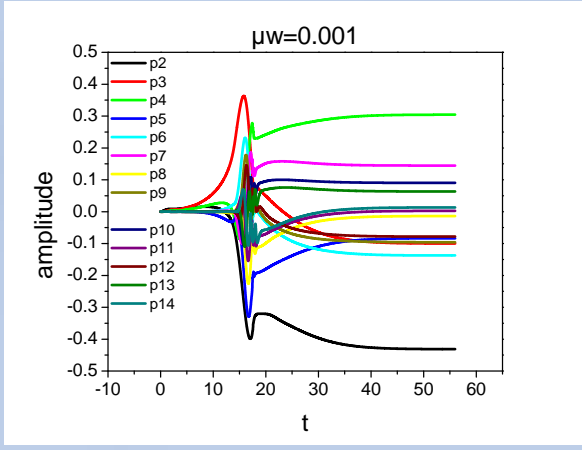
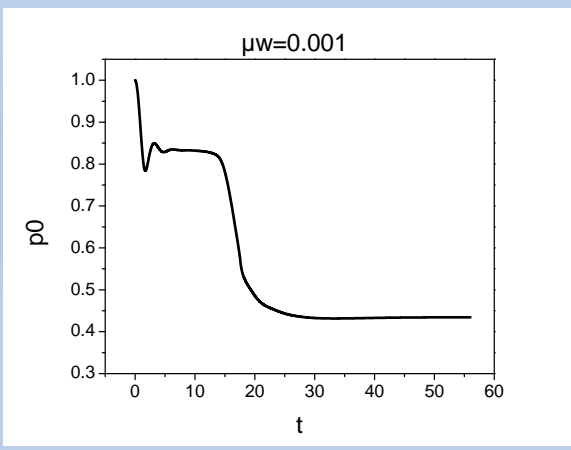
- Spine method fails to describe the bubble behavior all the way, whereas the elliptic mesh generation technique allow us to capture the deformation of the bubble at all stages.
- The bubble reaches again a static state of similar shape but much more compressed compared to the results in an unbounded flow.
- The wall presence accelerates the appearance of shape modes and alters slightly the final static shape. The movement of the bubble towards the wall is very small due to the viscosity of the liquid.

• Distance between the lower pole and the wall:

$$z_1 = 1$$

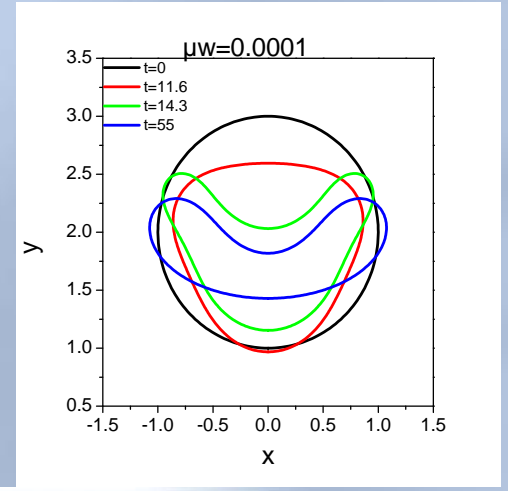
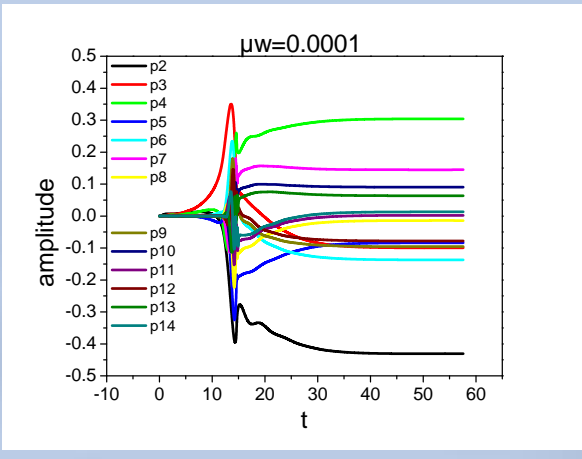
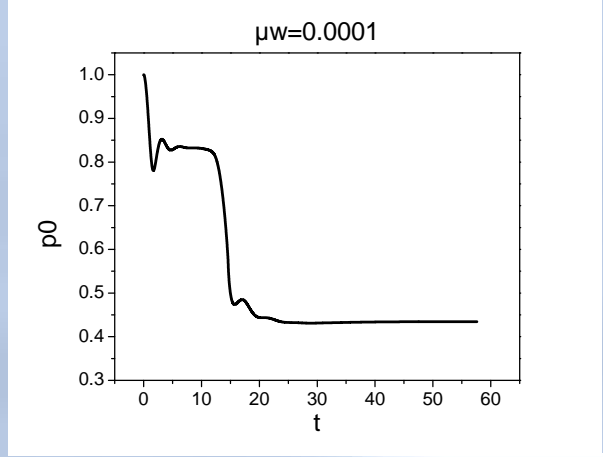
Viscosity of the surrounding liquid

$$\sim_w N 10^{>3} Pa \cdot s$$



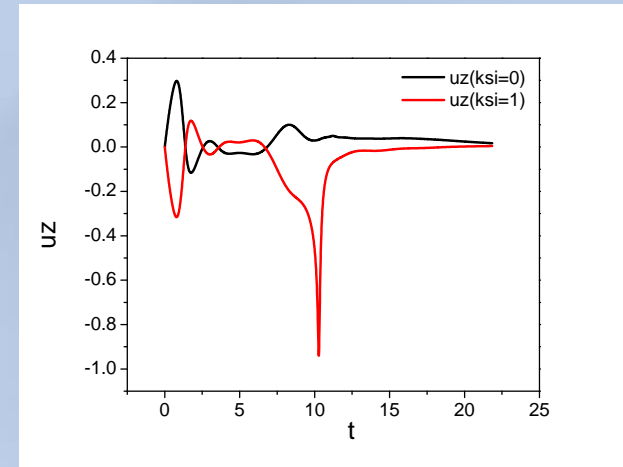
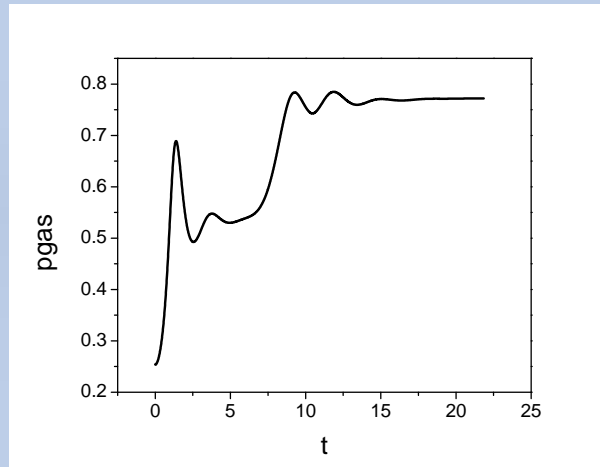
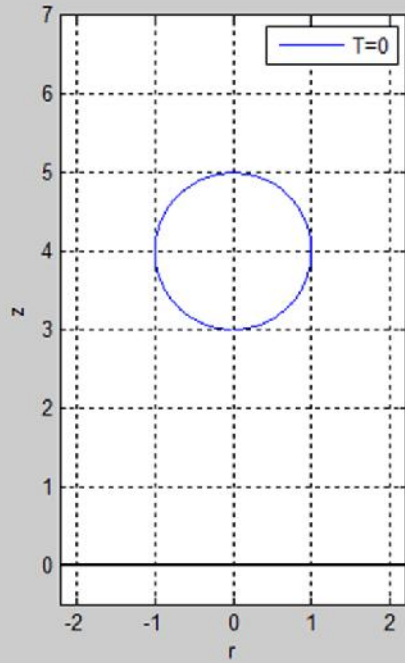
Viscosity of the surrounding liquid

$$\sim_w N 10^{>4} Pa \cdot s$$

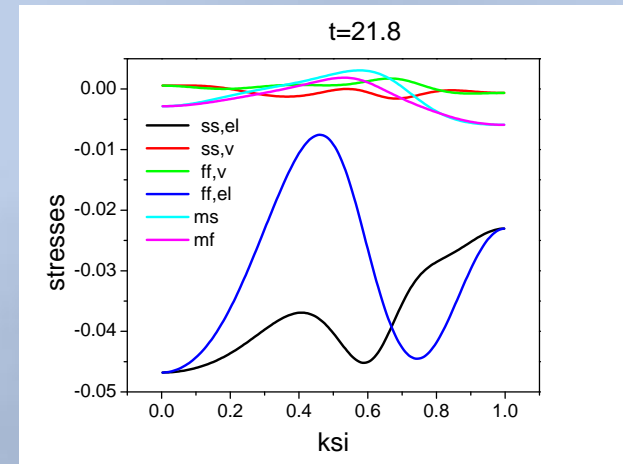
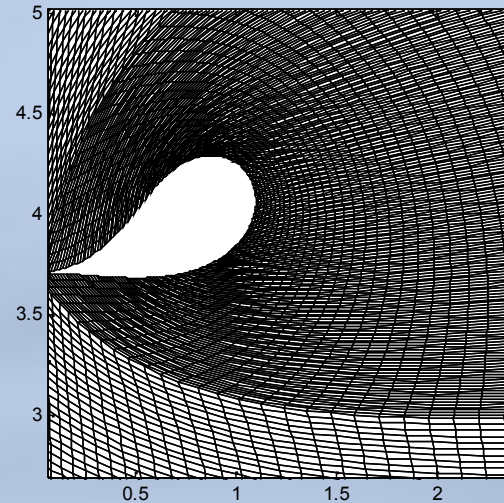


➤ If we reduce the distance between the bubble and the wall and/or the liquid viscosity we observe the same static state.

Imposition of greater disturbance: $P_{\infty}' = P_{st}' [1 + \nu], \nu = 3$



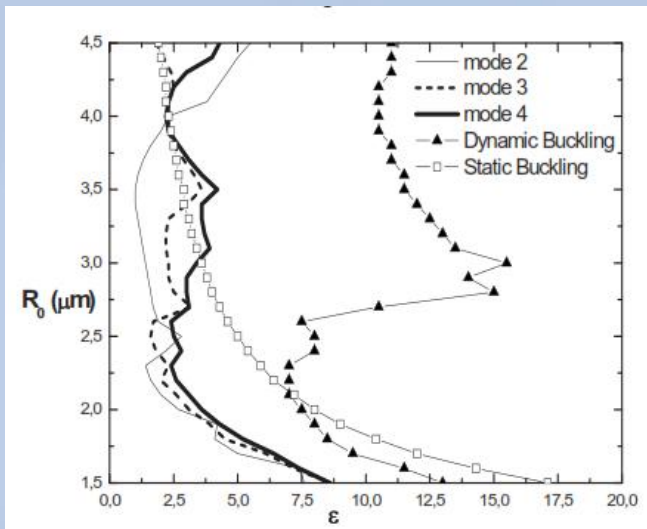
Final Mesh r-z



- For greater disturbances, static shapes are observed too – The poles of the bubble coalesce and a very compressed shape is formed compared to the results we obtain in the absence of the wall
- The upper pole is moving very fast inwards, then slows down and at the same time the lower pole starts moving upwards until the two poles coalesce

RESULTS FOR ACOUSTIC DISTURBANCES

- For acoustic disturbances, the behavior of contrast agents when there is no wall present is described by phase diagrams



(Tsigliferis & Pelekasis, 2011)

Region 1:

Amplitudes smaller than ϵ_{cr} for static buckling



Volume pulsations

Region 2:

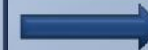
Amplitudes greater than ϵ_{cr} for static buckling and smaller than ϵ_{cr} for dynamic buckling



Shape oscillation in harmonic or subharmonic resonance

Region 3:

Amplitudes greater than ϵ_{cr} for dynamic buckling



Bubble collapse

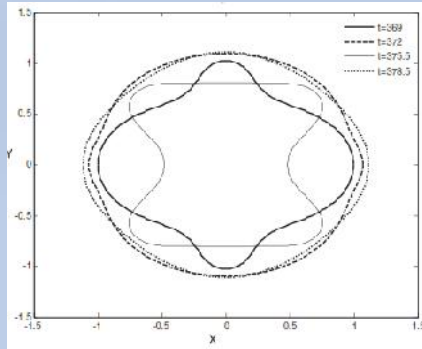
- We are interested in exploring dynamically if this behavior of contrast agents is influenced by the viscosity of the liquid and the wall presence.
- Furthermore, it is important to determine the mechanism of bubble collapse when the wall is present
- Finally, it is important to study the behavior of contrast agents near the wall where microstreaming is possible (Marmottant & Hilgenfeldt, 2003)

RESULTS FOR ACOUSTIC DISTURBANCES IN AN UNBOUNDED FLOW

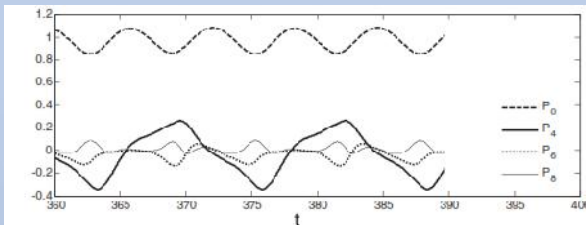
External disturbance:

$$P'_{\infty} = P'_{st} \left[1 + v \cos(\check{S}'_f t') \right], \quad f = 3.4 \text{ MHz}$$

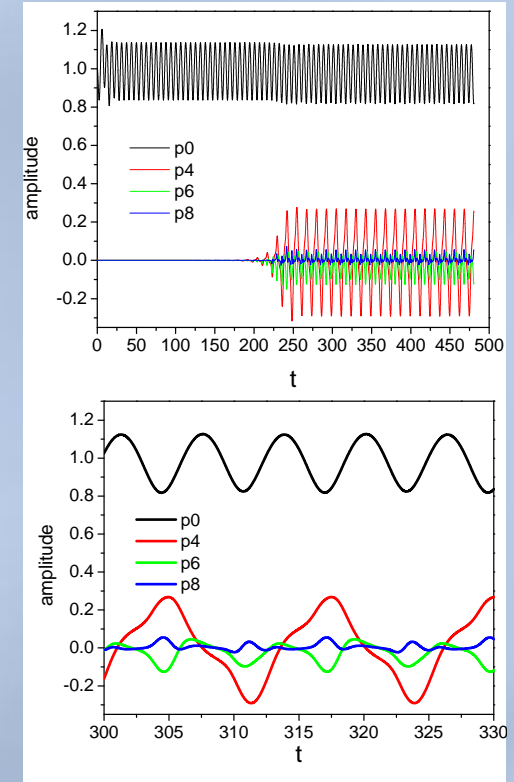
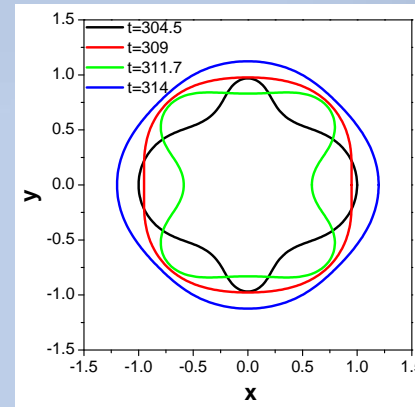
$$v = 5.1$$



(Tsiglifs & Pelekasis, 2013)



$$v = 7$$



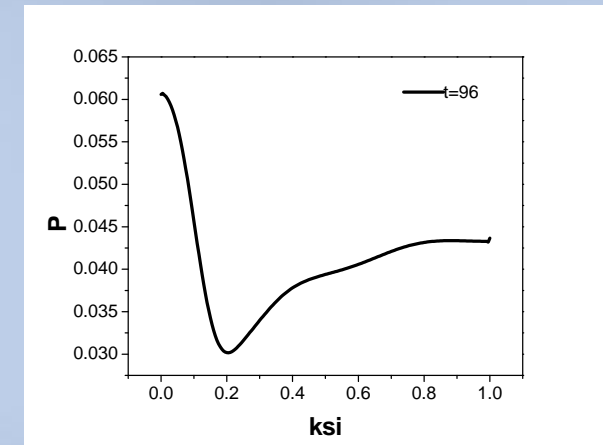
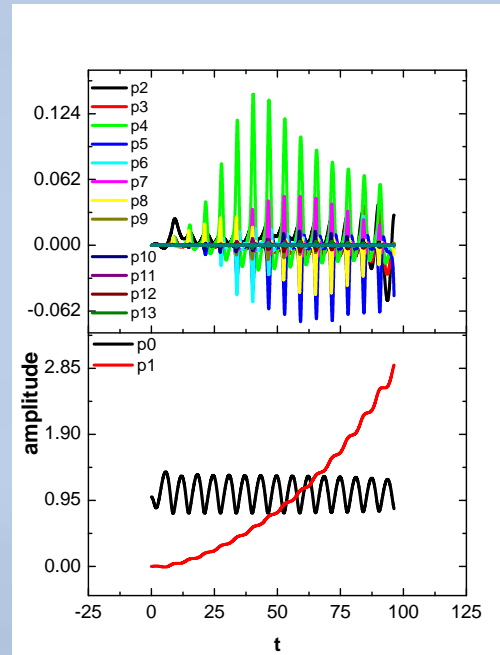
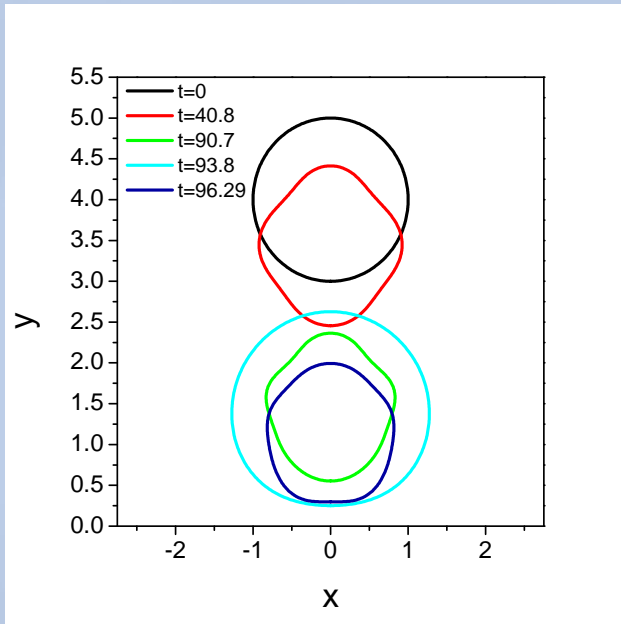
- For amplitude $\varepsilon=5.1$, we observe only volume and not shape oscillations when the viscosity of the liquid is accounted for.
- For amplitude $\varepsilon=7$, steady shape oscillations (P_4 dominates and P_6, P_8 follow) in subharmonic resonance (frequency of volume pulsations twice the frequency of P_4)
- Maximum mode amplitude when the bubble radius is minimum
- The viscosity alters the critical amplitude for dynamic buckling

RESULTS FOR ACOUSTIC DISTURBANCES FOR BUBBLE-WALL INTERACTION

$$P'_\infty = P'_{st} \left[1 + v \cos(\check{S}'_f t') \right], \quad f = 1.7 \text{ MHz}, \quad v = 3$$

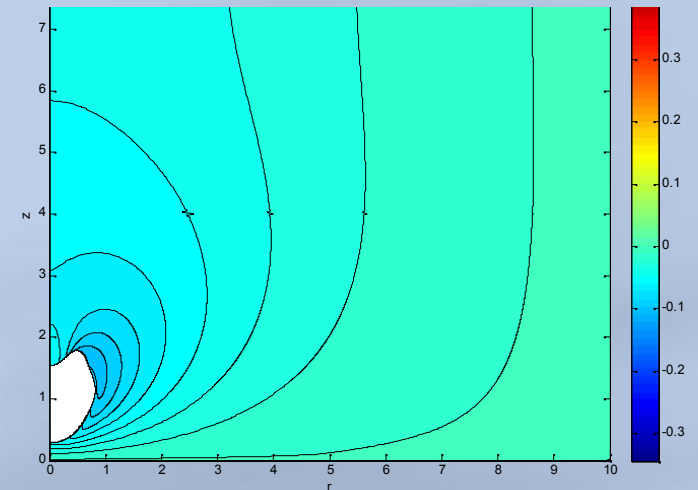
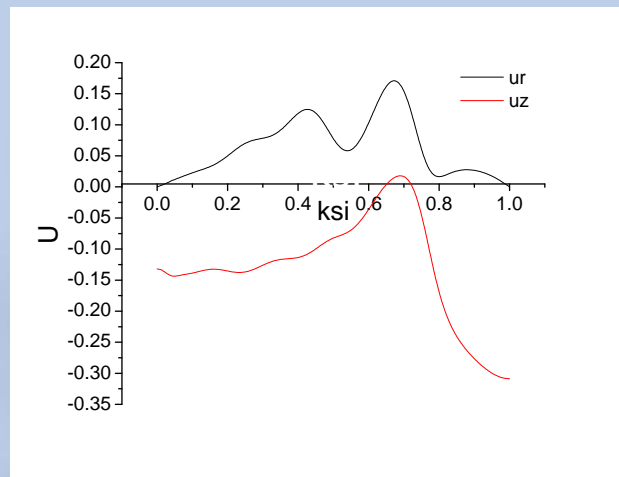
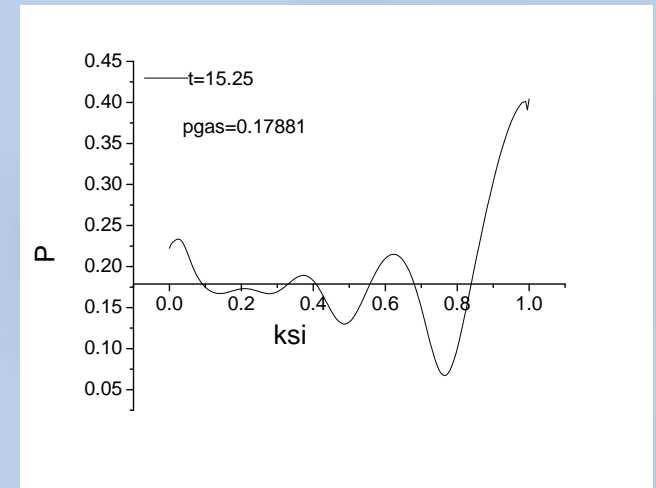
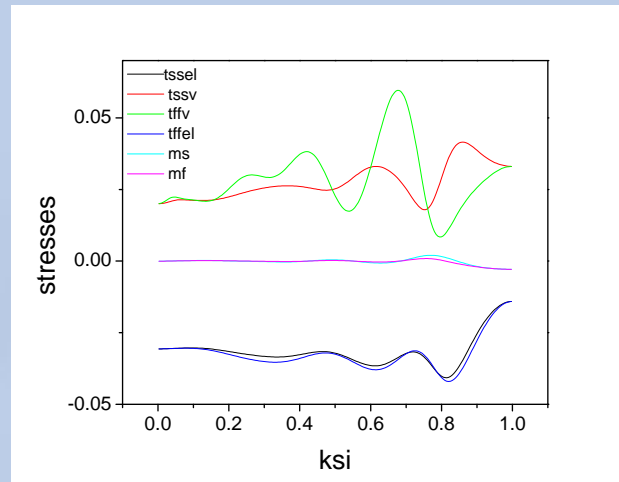
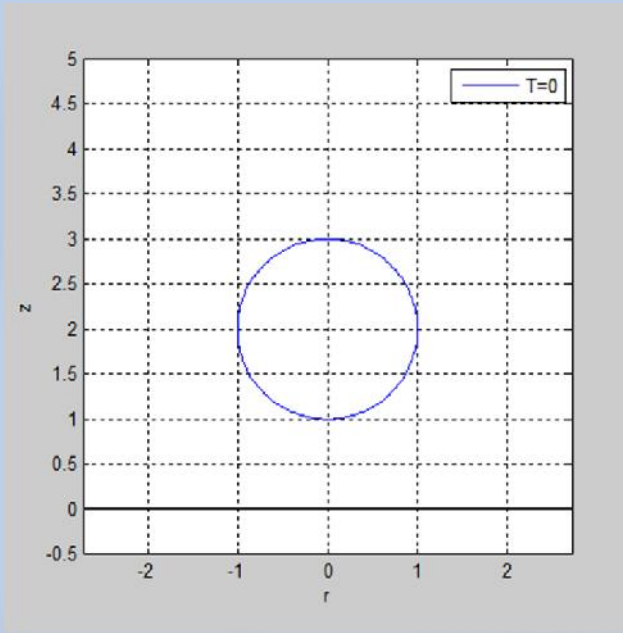
Surrounding liquid:
water ($\mu_l = 10^{-3} \text{ Pa}\cdot\text{s}$)

Distance between the lower pole and the wall: $z_1 = 3$



- The bubble oscillates with the frequency of the external disturbance and is moving towards the wall during compression.
- The shape during compression is elongated along the axis of symmetry. When the bubble reaches close to the wall, the liquid starts to resist the bubble movement and the shape eventually become straight and wide in the lower pole.
- There is a local pressure increase, lubrication pressure, in the region near the lower pole.

2. Liquid viscosity $\sim_w N 10^{>4} Pa \hat{n} s$



- If we reduce the viscosity of the liquid the bubble oscillations are more intense
- The bubble behave differently when it gets closer to the wall: the shape doesn't become wide and straight on the lower pole, but the upper pole starts moving inwards
- The bubble seems to collapse due to the viscous stresses of the membrane
- The microstreaming effect is captured

CONCLUSIONS

- We have developed a numerical methodology to simulate the dynamic behavior of contrast agents in a viscous flow by using a superparametric hybrid scheme that combines 2D lagrangian functions for the simulation of the liquid with 1D cubic splines to capture the shape of the membrane
- For the grid construction we have used and compared two methods : spine method and the elliptic mesh generation technique. The spine method fails to capture the large deformations of the bubble, especially in the presence of the wall. On the other hand, the elliptic method is able to follow the behavior of the bubble throughout all stages.
- For step change disturbances a steady non-spherical state is possible. If we ignore liquid viscosity or surface tension or if we don't permit the movement of the bubble the contrast agent collapses.
- The static arrangement is also observed in the presence of a rigid wall. The wall accelerates the appearance of shape modes and alters the final shape as it is much more compressed
- No jet formation was captured for the amplitudes of the step change disturbances we have used.

- For acoustic disturbances the bubble oscillates with the frequency of the external disturbance and moves towards the wall during compression. The viscosity of the surrounding liquid alters the critical amplitude for dynamic buckling.
- For the case of water, when the bubble reaches very close to the wall the liquid starts to resist its movement, the shape becomes straight and wide in the lower pole as a result of the development of lubrication pressure in that region.
- For viscosities smaller than water, a different behavior is captured. The shape doesn't become wide and straight on the lower pole, but the upper pole starts moving inwards and eventually the bubble seems to collapse due to the viscous stresses of the membrane.
- The microstreaming effect was captured which has important implications in mass transfer of surface material or material placed inside the microbubble, towards nearby surfaces



AKNOWLEDGMENTS

This work was co-financed from the Greek General Secretariat for Research and Technology and from European union through the program ARISTEIA I